

Fig.2 Trajectory coordinate system definition in the y-direction,

$$F_a = \frac{1}{2} C_D \rho_a A_d V_{res}^2 \quad (1)$$

The component of this force acting in the x-direction is

$$\begin{aligned} F_{ax} &= \frac{1}{2} C_D \rho_a A_d V_{res}^2 \cos \gamma \\ &= \frac{1}{2} C_D \rho_a A_d V_{res} u_{rel} \end{aligned} \quad (2)$$

Taking u_d as the component of the droplet velocity in the x-direction, F_{ax} as the component of the aerodynamic force in the x-direction, F_{gx} as the component of the gravitational force in the x-direction, A_d as the frontal area of the droplet, D as the droplet diameter, g as the acceleration due to gravity, ρ_d as the droplet density (1000 kg m^{-3} for water), ρ_a as the air density, m_d as the droplet mass, c as the aerofoil chord, C_D as the drag coefficient for the droplet, the following expression for the acceleration in the x-direction (in m s^{-1}) may be derived:

$$\frac{du_d}{dt} = \frac{F_{ax} + F_{gx}}{m_d} \quad (3)$$

Using the following expressions,

$$m_d = \rho_d \times \frac{4}{3} \pi \frac{1}{8} D^3$$

$$A_d = \frac{1}{4} \pi D^2,$$

$$F_{gx} = m_d g \left(1 - \frac{\rho_a}{\rho_d} \right) \sin(\alpha - \phi), \quad (4)$$

$$\frac{du_d}{dt} = \frac{\frac{1}{2} C_D \rho_a \pi \frac{1}{4} D^2 V_{res} u_{rel}}{\frac{4}{24} \rho_d \pi D^3} +$$

$$\frac{m_d g}{m_d} \left(1 - \frac{\rho_a}{\rho_d} \right) \sin(\alpha - \phi)$$

This can be further simplified by making a substitution using the droplet Reynolds number

$$R = \frac{\rho_a V_{res} D}{\mu} \quad (5)$$

$$\frac{du_d}{dt} = \frac{18 C_D R \mu u_{rel}}{24 \rho_d D^2} + \left(1 - \frac{\rho_a}{\rho_d} \right) g \sin(\alpha - \phi) \quad (6)$$

which are written in a non-dimensional form using

$$\bar{u}_d = \frac{u_d}{V_\infty}, \quad \bar{t} = \frac{t V_\infty}{c}, \quad \bar{u}_{rel} = \frac{u_{rel}}{V_\infty}$$

$$\frac{d\bar{u}_d}{d\bar{t}} \times \frac{V_\infty^2}{c} = \frac{18 C_D R \mu \bar{u}_{rel} V_\infty}{24 \rho_d D^2}$$

$$+ \left(1 - \frac{\rho_a}{\rho_d} \right) g \sin(\alpha - \phi) \text{ astfel ca}$$

$$\frac{d\bar{u}_d}{d\bar{t}} = \frac{18 C_D R \mu \bar{u}_{rel}}{24 \rho_d D^2 V_\infty}$$

$$+ \left(1 - \frac{\rho_a}{\rho_d} \right) \frac{c}{V_\infty^2} g \sin(\alpha - \phi). \quad (7)$$

Similarly,

$$\frac{d\bar{v}_d}{d\bar{t}} = \frac{18 C_D R \mu \bar{v}_{rel}}{24 \rho_d D^2 V_\infty}$$

$$- \left(1 - \frac{\rho_a}{\rho_d} \right) \frac{c}{V_\infty^2} g \cos(\alpha - \phi).$$

Furthermore, introducing the inertia parameter

$$K = \frac{\rho_d D^2 V_\infty}{18 \mu c}$$

result

$$\frac{d\bar{u}_d}{d\bar{t}} = \frac{C_D R \bar{u}_{rel}}{24 K}$$

$$+ \left(1 - \frac{\rho_a}{\rho_d} \right) \frac{c}{V_\infty^2} g \sin(\alpha - \phi) \quad (8)$$

$$\frac{d\bar{v}_d}{d\bar{t}} = \frac{C_D R \bar{v}_{rel}}{24 K}$$

$$- \left(1 - \frac{\rho_a}{\rho_d} \right) \frac{c}{V_\infty^2} g \cos(\alpha - \phi)$$

The equations of motion are readily solved using Runge-Kutta or similar numerical methods, with the initial droplet velocity at the trajectory starting point several chord lengths ahead of the body usually assumed to be the same as that of the aerodynamic flow.

Flow solution

With panel methods, the flow solution is evaluated at each position of the droplet trajectory by

summing the contribution to the flow from the calculated circulation from a series of panels that describe the aerofoil or body profile. The flow solution at the surface of the profile is also required in the accretion analysis.

The alternative is a grid-based solution in which the velocity is known at discrete node points of a grid around the body. The velocity at a given point in space is then estimated by interpolation using the surrounding grid nodes.

We consider a control volume located on the surface of the body and which extends from outside the boundary-layer to the surface.

The lower boundary of the control volume is initially on the surface of the clean geometry and moves outward with the surface as the ice accretes. Computationally a control volume is placed over each panel defining the body geometry as shown in fig 3.

The conservation of mass requires that the mass flow rate entering the control volume is equal to the mass flow rate leaving the control volume, that is:

$$\dot{m}_c + \dot{m}_{r_{in}} = \dot{m}_i + \dot{m}_e + \dot{m}_{r_{out}} \quad (9)$$

Here \dot{m}_c is the mass flow rate of the impinging water entering the control volume and $\dot{m}_{r_{in}}$ is the mass flow rate of the water along the surface exiting from the adjacent upstream control volume. The leaving mass flow rates consist of the "accumulated ice", \dot{m}_i , loss through evaporation, \dot{m}_e , and water flowing out of the control volume, $\dot{m}_{r_{out}}$. The three mass flow rates \dot{m}_i , \dot{m}_c , and $\dot{m}_{r_{in}}$ are related to each other by the concept of freezing factor f , defined as the fraction of the total mass flow rate of water entering the control volume that freezes,

$$f = \frac{\dot{m}_i}{\dot{m}_{c_i} + \dot{m}_{r_{in}}} \quad (10)$$

Solving for \dot{m}_i and substituting the resulting expression into the value of $\dot{m}_{r_{out}}$ can be obtained from:

$$\dot{m}_{out} = (\dot{m}_c + \dot{m}_{r_{in}})(1 - f) - \dot{m}_e \quad (11)$$

once f , \dot{m}_c , $\dot{m}_{r_{in}}$ and \dot{m}_e are known.

The equation (11) is applied to each surface element on the airfoil where ice accumulates. Calculations start from the stagnation point where $\dot{m}_{in} = 0$, because of symmetry and proceed in the downstream direction on both upper and lower surfaces.

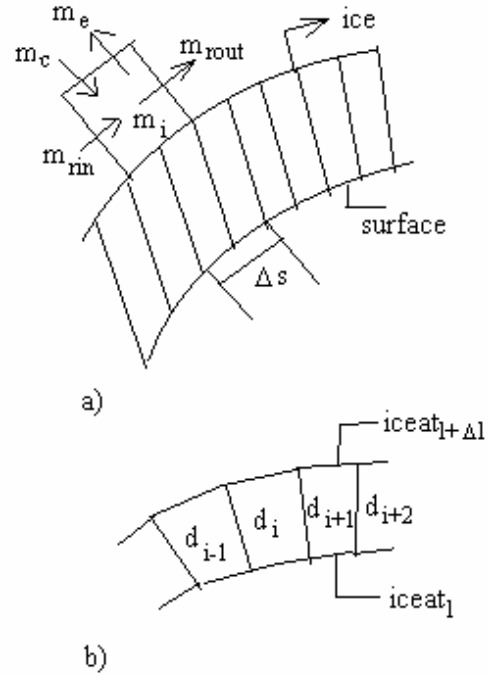


Fig.3. Control volume for the energy balance (a) single control volume on the icing surface, (b) control volumes over each panel which defines the airfoil geometry

At the first surface element, for an assumed f , equation (11) contains only one unknown quantity, which is $\dot{m}_{r_{out}}$ since \dot{m}_c is computed from corresponding equations [1]. At the next surface element $\dot{m}_{r_{out}}$ of the first segment becomes \dot{m}_{in} for the second segment and with \dot{m}_c and \dot{m}_e computed [1] as before, $\dot{m}_{r_{out}}$ is computed from eq. 11 and this process is repeated for each surface segment.

The energy balance is applied to the control volume by using the first law of thermodynamics which requires that the energy inflow rate is equal to the energy outflow rate. Application of the energy balance to the control volume of Fig.3 gives:

$$\dot{m}_c H_{t,T_\infty} + \dot{m}_{r_{in}} H_{w,s_{i-1}} + \dot{q}_k \Delta s = \dot{m}_e H_{v,s} + \dot{m}_i H_{i,s} + \dot{m}_{ext} H_{w,s_i} + \dot{q}_C \Delta s \quad (12)$$

The equations (11) and (12) are solved iteratively.

The thickness of boundary ice is:

$$\Delta y = \frac{\dot{m}_i}{\rho_i} \quad (13)$$

These Δy increments are then added to the original surface segments as to create a new airfoil on which the ice accumulation calculations are repeated for the Δt next time interval.

Thus, calculations for each step involves recomputing the inviscid flow, determining impingement pattern for the new configuration, and reevaluating the heat balance equation. Numerical calculation includes the phases:

- 1) read the initial coordinates, x, z , of the considered airfoil profile and the speed distribution U_e is computed for the airfoil with the panels method;
- 2) the dynamical and thermal boundary layer equations are solved, resulting:

$$\bar{U} \text{ and } \bar{\Delta T};$$

- 3) with (5.16) the ice thickness for the first time step is calculated;
- 4) the new coordinates of airfoil profile are calculated;

The (1) step is repeated.

Conclusions

The phenomenon of ice accretion over the airfoil profile is the effect of a triplet : the mass of water droplets (from cloud), the air fluid motion over the airfoil profile and the solid surface. These interactions are controlled by many factors, who are defined as parameter:

- the pressure, the temperature and humidity of the environment.
- the speed and direction of air stream ;
- the physical and chemical of cloud mass (the density and chemical composition of cloud)
- the interaction between water droplet and airstream (the buoyancy force, the friction force) that are determined by V_∞, ρ_d, K .
- the interaction between the water droplets and the phenomenon from dynamic and thermal boundary layer ($U_e, \bar{U}, \bar{\Delta T}$), the mass and energy transfer, free and forced convection;
- the interaction between the droplets and the solid surface of the airfoil profile semi-elastic interaction (the efficiency of droplets adhesion at the airfoil surface).

With the considered mathematical model, a numerical code simulating the process of ice accretion over the airfoil is elaborated. The form and mass of ice deposition over the aerodynamic airfoil are functions of $R_d/R_\infty, \tau, e = b/a, \alpha=0$. The calculation is done for laminar and incompressible flow around the aerodynamic profiles described in Anexe 1 and the results are represented in the following figures in Anexe 2:

Fig.1 $R_d/R_\infty : (0.45, 0.55, 0.65, 0.75, 0.85, 0.95)$; $\tau = 0.25$; $e = b/a : (1, 0.5, 0.25, 0.125)$

Fig. 2 $\tau : (0.01, 0.05, 0.1, 0.15, 0.2, 0.25)$, $R_d/R_\infty = 0.85$, $e = b/a : (1, 0.5, 0.25, 0.125)$

Fig.3 $\Delta T: (0.005, 0.1, 0.3, 0.5, 0.7)$; $R_d/R_\infty = 0.85$; $e = b/a : (1, 0.5, 0.25, 0.125)$

Fig.4 \bar{U} the influence of dynamic and thermal boundary layer $\bar{\Delta T}$, about ice accretion

simulation $\tau : (0.01, 0.05, 0.1, 0.15, 0.2, 0.25)$ $R_d/R_\infty = 0.85$.

Fig.5 The simultaneous influence of Kr (roughness), \bar{U} , of dynamic and thermal boundary layer $\bar{\Delta T}$; $\tau : (0.01, 0.05, 0.1, 0.15, 0.2, 0.25)$, $R_d/R_\infty = 0.85$.

Fig.6 The simultaneous influence of Kr (roughness), \bar{U} , of dynamic and thermal boundary layer $\bar{\Delta T}$ for aerodynamic profiles; $\tau : (0.01, 0.05, 0.1, 0.15, 0.2, 0.25)$, $R_d/R_\infty = 0.85$.

REFERENCES

- [1] *CEBECI, T., "An Engineering Approach to the calculation of Aerodynamic Flows"*; Springer, 1999.
- [2] *R.W. GENT, N.P. DART and J.T. CANSDALE, "Aircraft Icing"*, Phil. Trans. R. Soc. London A (2000) 358, 2873-2911.
- [3] *SANDER J. JACOBS, JACCO M. HOSPERS, HARRY W.M. HOEIJMAKERS*, University of Twente Enschede, the Netherlands, 26TH International Congress of the Aeronautical Sciences, 2008.

Anexa I

Thin profile

$$z(x) = h \begin{pmatrix} 0.1969\sqrt{x} - 0.126x - \\ 0.2537x^2 + 0.2843x^3 \\ - 0.1015x^4 \end{pmatrix}$$

for $h=1$.

$$z(x) = -h \begin{pmatrix} 0.2969\sqrt{x} - \\ 0.226x - 0.4537x^2 + \\ 0.4843x^3 - 0.1015x^4 \end{pmatrix}$$

for $h=1$.

Thick profile

$$z(x) = h \begin{pmatrix} 0.2969\sqrt{x} - 0.126x \\ - 0.3537x^2 + 0.2843x^3 \\ - 0.1015x^4 \end{pmatrix}$$

$$z(x) = h \begin{pmatrix} 0.4969\sqrt{x} - 0.426x \\ - 0.4537x^2 + 0.4843x^3 \\ - 0.1015x^4 \end{pmatrix}$$

Anexa II

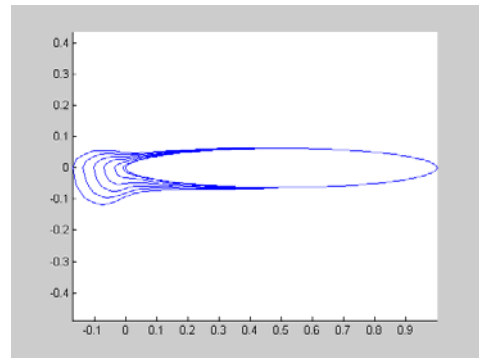
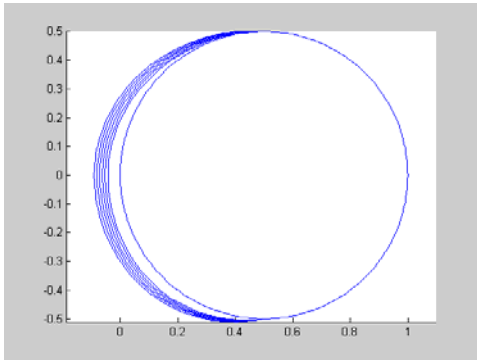


Fig.2

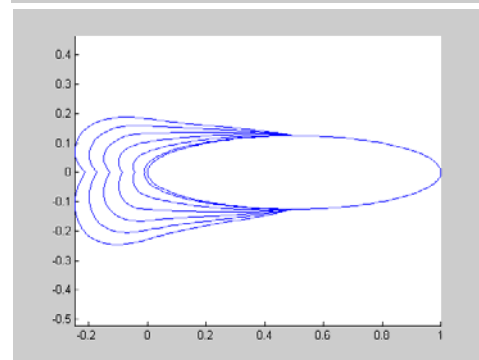
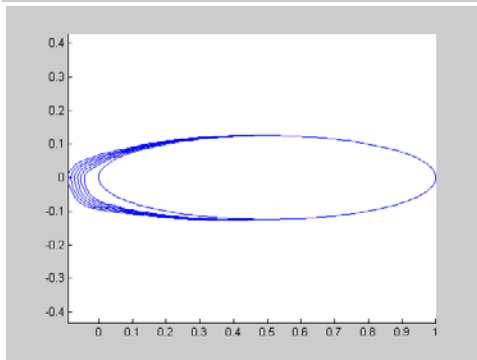
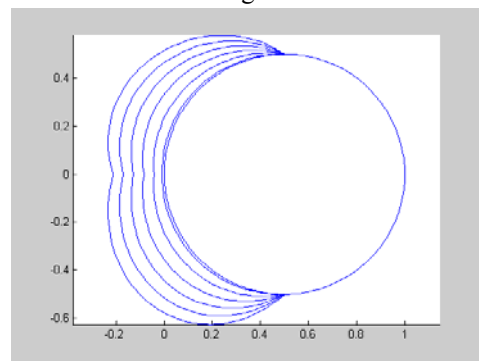
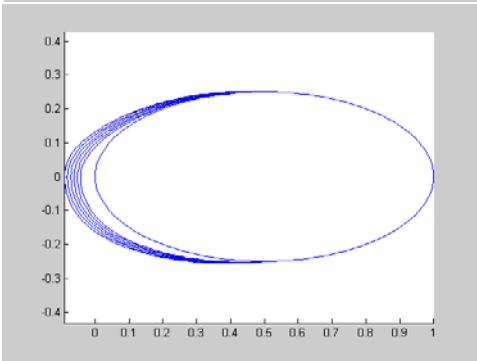


Fig.1

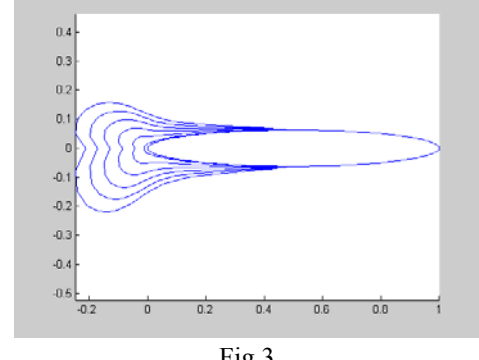
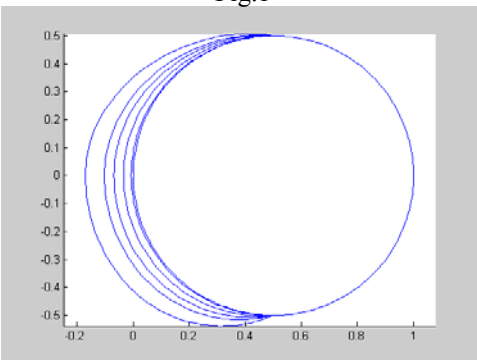
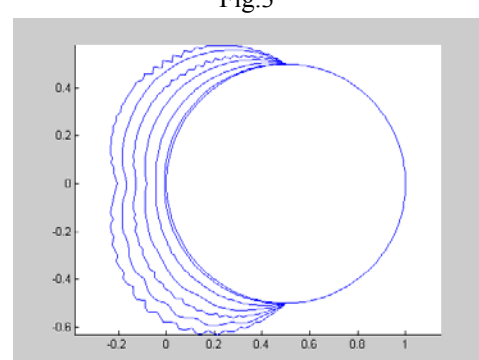
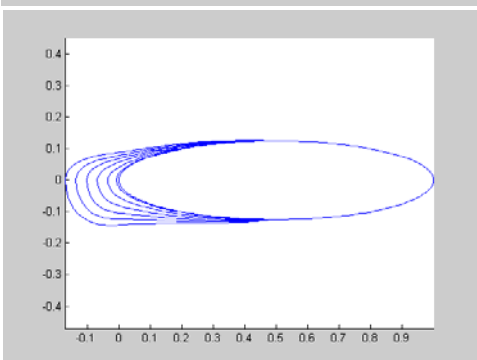


Fig.3



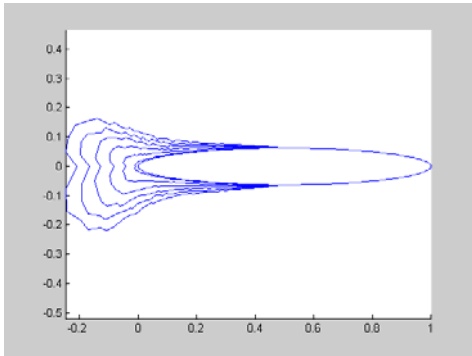
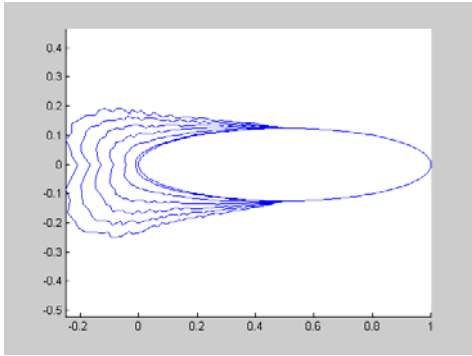


Fig.4

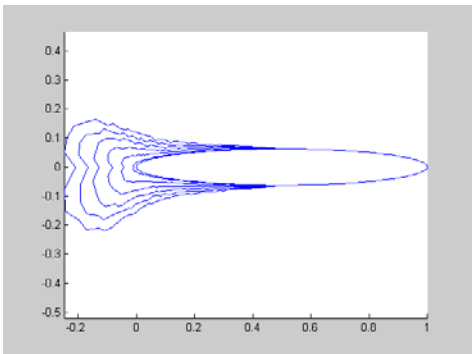
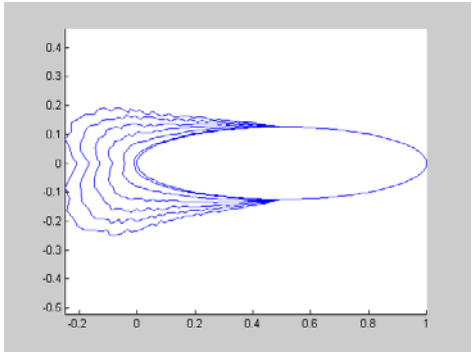
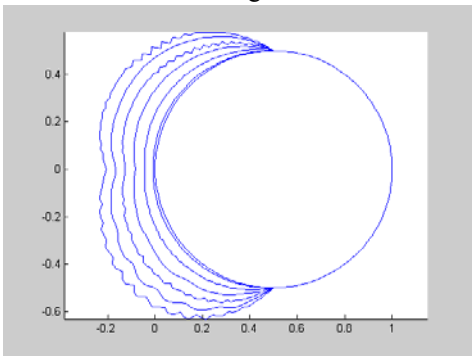


Fig.5

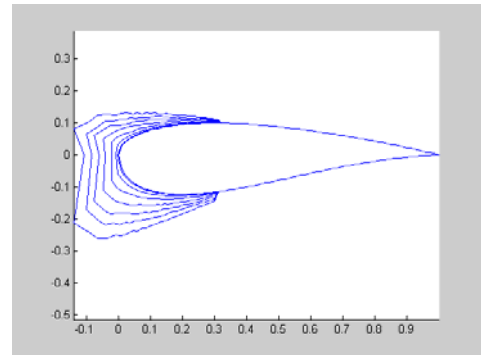
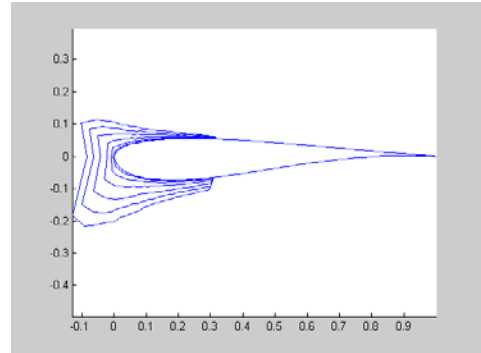


Fig.6